CHAPTER FIVE

In vitro production of N-degron fused proteins and its application

Bong Heon Kim, Do Hoon Kwon[†], Leehyeon Kim[‡], Woo Seok Yang, and Hyun Kyu Song*

Department of Life Sciences, Korea University, Seoul, South Korea
*Corresponding author: e-mail address: hksong@korea.ac.kr

Contents

1. Introduction 100
2. Key resources 105
   2.1 Key resources table 105
   2.2 Materials 107
   2.3 Buffer recipes 108
3. Preparation of N-degron attached ZZ-domain of p62/SQSTM1 108
   3.1 Molecular cloning LC3B fused human p62 ZZ-domain 108
   3.2 Expression of N-degron fused ZZ-p62 110
   3.3 Purification of N-degron fused ZZ-p62 112
4. Preparation of human ATG4B protease 115
   4.1 Purification of human ATG4B 115
5. Applications of N-degron fused ZZ-p62 or N-degron fused proteins of interest 116
   5.1 Crystallization of REEED-ZZ p62 116
   5.2 Notes 116
   5.3 Structure determination 116
   5.4 Other applications of LC3B-fusion technique 119
6. Conclusions 119
Acknowledgments 119
References 120

Abstract

The N-degron pathway, first discovered several decades ago by Varshavsky's laboratory, controls the half-life of target proteins depending on their N-terminal residues. *In vivo* cell biology studies have established the physiological role of the N-degron pathway.

[†] Present address: Department of Biochemistry, Duke University School of Medicine, Durham, NC 27710, United States.
[‡] Present address: Cell Biology Program, Memorial Sloan Kettering Cancer Center, New York, NY 10065, United States.

Methods in Enzymology, Volume 686
ISSN 0076-6879
https://doi.org/10.1016/bs.mie.2023.02.002

However, *in vitro* studies such as biochemical assays and structural biology studies are relatively limited. The N-degron substrates cannot be obtained *via* simple protein expression. The N-degron residues are exposed *via* the proteolytic process from the translated nascent polypeptide chains. Thus, methods for the fusion expression with several cleavable tags and subsequent treatment with specific proteases to design the exposed N-degron signals have been introduced. Recently, we developed a unique fusion technique using microtubule-associated protein 1A/1B light chain 3B (LC3B), a key marker protein of autophagy, to obtain a high yield of the purified target proteins with variable N-terminal residues for various biochemical studies including enzymatic and binding assays, and crystallization of N-degron complex. This chapter describes the protocols that include the vector map designed for producing LC3B fused target proteins, methods for expression and purification of an example protein, p62/SQSMT1, using different N-terminal residues, and methods to obtain the purified ATG4B protease, which is used for processing LC3B tag and exposing the required N-terminal residues of the target protein.

1. Introduction

The N-degron pathway (formerly the N-end rule pathway) is a proteolytic process that targets the N-terminal residues of proteins and affects their half-life (Varshavsky, 2019). The N-degron pathway has been extensively studied; depending on the N-terminal residues, several different N-degron pathways, such as the Arg/N-degron, Ac/N-degron, Pro/N-degron, Gly/N-degron, and fMet/N-degron pathways, govern the fate of substrate proteins (Bachmair, Finley, & Varshavsky, 1986; Bachmair & Varshavsky, 1989; Baker & Varshavsky, 1995; Balzi, Choder, Chen, Varshavsky, & Goffeau, 1990; Cha-Molstad et al., 2015; Chen, Kim, Song, & Varshavsky, 2021; Chen, Wu, Wadas, Oh, & Varshavsky, 2017; Hu, Wang, Xia, & Varshavsky, 2008; Hwang, Shemorry, & Varshavsky, 2010; Hwang & Varshavsky, 2008; Kim et al., 2014, 2018; Piatkov, Vu, Hwang, & Varshavsky, 2015; Shemorry, Hwang, & Varshavsky, 2013; Tasaki & Kwon, 2007; Varshavsky, 2008, 2019). However, in contrast to cell biology studies of the N-degron pathway, *in vitro* studies, such as biochemical assays and structural biology studies, were relatively few until recently (Cha-Molstad et al., 2017; Chen et al., 2021; Choi et al., 2010; Chrustowicz et al., 2022; Dong et al., 2018, 2020; Kim et al., 2021, 2022; Kim, Kwon, Heo, Park, & Song, 2020; Kim, Oh, Lee, & Song, 2016; Kwon et al., 2018; Kwon, Kim, & Song, 2019; Matta-Camacho, Kozlov, Li, & Gehring, 2010; Munoz-Escobar, Kozlov, & Gehring, 2017; Pan et al., 2021; Qiao et al., 2020; Sherpa, Chrustowicz, & Schulman, 2022). Therefore, to understand

the specificity of the molecular interaction between N-degron and its recognition component, N-recognin, *in vitro* study using the protein sample is inevitable.

When amino acids at the N-terminus are exposed, they are recognized and processed for degradation by proteins such as N-recognins or N-terminal modifying enzymes (Aksnes, Drazic, Marie, & Arnesen, 2016; Kim et al., 2022; Kim, Oh, et al., 2016; Pan et al., 2021; Van Damme et al., 2022). The binding pockets of these proteins are diverse in shape, which confers on them the specificity for the target sequence at the N-termini. Thus, proteins possessing a homogeneous N-degron sequence at the N-terminus must be produced; however, many obstacles exist. The protein translation must start with methionine. Although methionine aminopeptidases (MetAPs) cleave the first methionine in most of the mature proteins, the efficiency of these proteases differs depending on the second residue, resulting in heterogeneous proteins (Nguyen, Kim, Park, & Hwang, 2019; Xiao, Zhang, Nacev, Liu, & Pei, 2010). Furthermore, many proteases conventionally used in tag cleavage require unique sequences for their specificity and efficiency. The residual sequence after cleavage is very confined, which hinders its ability to participate in all the N-degron pathways. Native chemical ligation also can be used to construct the desired sequence at the N-terminus, which attaches the peptides with the target sequence to the proteins' N-terminus (Berrade & Camarero, 2009; Pan et al., 2021). Regardless, this method may be difficult to perform in laboratories that do not typically study chemical reactions. Ubiquitin (Ub) or small ubiquitin-like modifier (SUMO) can be employed as N-terminal tagging proteins for exposing desired amino acids at the N-terminus (Bachmair et al., 1986; Baker, 1996; Satakarni & Curtis, 2011). Ub enhances protein yield, and deubiquitylating enzymes (DUBs) are particular to the cleavage of the Ub tag. However, most DUBs are relatively large enzymes, and therefore hard to purify in large quantities using an inexpensive *E. coli* expression system. Furthermore, Ub has a comparatively short-length linker of about 5 amino acids long in the C-terminal, leading to low cleavage efficiency by protease when used as a tag at the N-terminal side of the target protein. SUMO-specific proteases show high efficiency in removing the tag from the target protein, even in smaller quantities; however, their large-scale production remains difficult (Kim et al., 2020). SUMO also has chaperone-like properties, helping fused proteins fold correctly and achieve a higher expression level. However, in some cases, SUMO fusion proteins go to inclusion bodies, for which different processes, such as

refolding, are required; this results in insufficient samples for further experiments.

For these reasons, we developed the protein tag using microtubule-associated protein 1A/1B light chain 3B (LC3B) for expressing target proteins with the desired sequence in the N-terminal region (Kim et al., 2020). This LC3B-fusion method is advantageous in N-degron studies, mainly carried out *in vitro*. LC3B is one of the proteins in LC3-family, which comprises LC3A, LC3B, and LC3C, and is used in autophagy as a structural protein of the autophagosomal membrane (Kim, Kwon, & Song, 2016; Kwon et al., 2017; Nakatogawa, Suzuki, Kamada, & Ohsumi, 2009; Noda, Ohsumi, & Inagaki, 2010; Park et al., 2022; Schaaf, Keulers, Vooijs, & Rouschop, 2016). LC3s are the Ub-like modifier analogous to ubiquitylation, which is conjugated *via* the C-terminal glycine to phosphatidylethanolamine (PE) in the autophagosome (Hong, Kim, Kim, & Song, 2012; Hong et al., 2011; Metlagel, Otomo, Ohashi, Takaesu, & Otomo, 2014; Ohsumi, 2001). During autophagosome formation, the C-terminal region of LC3s is cleaved by the cysteine protease ATG4B, exposing C-terminal glycine (Kwon et al., 2017; Maruyama & Noda, 2017; Ohsumi, 2001; Satoo et al., 2009; Tanida, Ueno, & Kominami, 2004). Then, the noncanonical E1-like enzyme ATG7 activates the processed LC3s *via* an ATP-dependent manner to conjugate LC3s with PE along with ATG3, which acts as an E2-like enzyme for this reaction (Tanida et al., 2004). PE-conjugated LC3s are also deconjugated by ATG4B for recycling and further autophagy (Kwon & Song, 2018; Satoo et al., 2009). The interaction between LC3s and ATG4B is robust and diverse. ATG4B not only cleaves LC3s from peptides and proteins but also deconjugates LC3s from the lipid PE (Maruyama & Noda, 2017).

Upon using this versatility to target molecules of the LC3s-ATG4B system, we found that the LC3B present before all 20 canonical amino acids except proline can be processed to produce proteins of interest with different N-terminal residues (Fig. 1). From the previously solved crystal structure of LC3B (Kwon, Kim, Jung, et al., 2017; Kwon, Kim, Kim, et al., 2017; Noda et al., 2010), we found that this protein has a longer C-terminal tail (12 residues long) than Ub, which helps efficient processing by proteases. More importantly, the ATG4B protease can be overexpressed using the *E. coli* expression system and purified homogeneously with ease (Kwon, Kim, Jung, et al., 2017; Satoo et al., 2009). Therefore, we can obtain a large quantity of active ATG4B protease, which must be economically

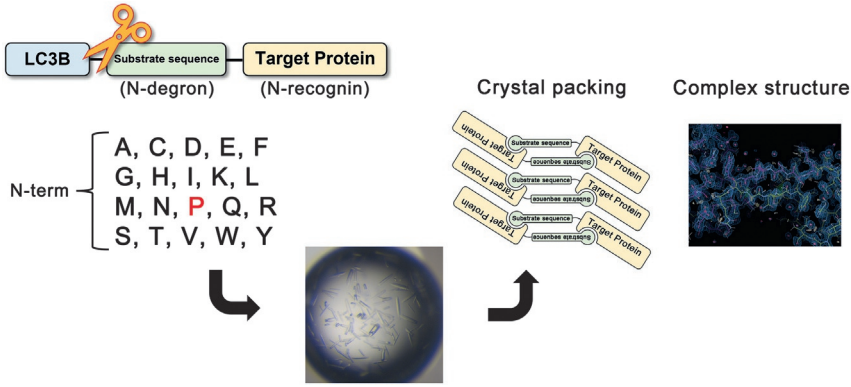

Fig. 1 Overall scheme of the LC3B-fusion technique. The construct comprises LC3B-[N-degron sequence]-target protein (usually N-recognin). ATG4B (scissor) cleaves the peptide bond between the C-terminus of LC3B (glycine) and substrate sequences except for at a proline residue. These N-degron fused N-recognins have been widely used for successful crystallization. The N-degron residues bind to neighboring target proteins in the crystalline lattice. Representative electron density map showing the structure in complex with N-degron.

compared with other commercially available Ub- or SUMO-proteases. ATG4B cannot process LC3B immediately after proline, but the MetAP cotranslationally processes the first methionine, and the proline is exposed at the N-terminus of the target protein without the tagging system (Shin, Park, Kim, Heo, & Song, 2021). Therefore, it allows us to express the proteins with all 20 different amino acids at the N-termini.

In this chapter, we provide the vector map designed for convenient cloning and expression of the LC3B fusion protein (Fig. 2) and describe key resources, experimental procedure for cloning, expression, and purification of the protein of interest in Sections 2 and 3. The 6× tandem His residues, commonly used for affinity chromatography, were inserted into the N-terminal side of the LC3B tag of the expression vector for efficient purification and the removal of LC3B after ATG4B cleavage. The detailed method for expression and purification of ATG4B protease is also included in Section 4. Furthermore, the applications of the LC3B-fusion technique for N-degron research, including crystallization and structure determination, are introduced in Section 5. Although the concepts and examples of this technique have been reported previously (Kim et al., 2020), the detailed experimental procedure is described in this chapter.

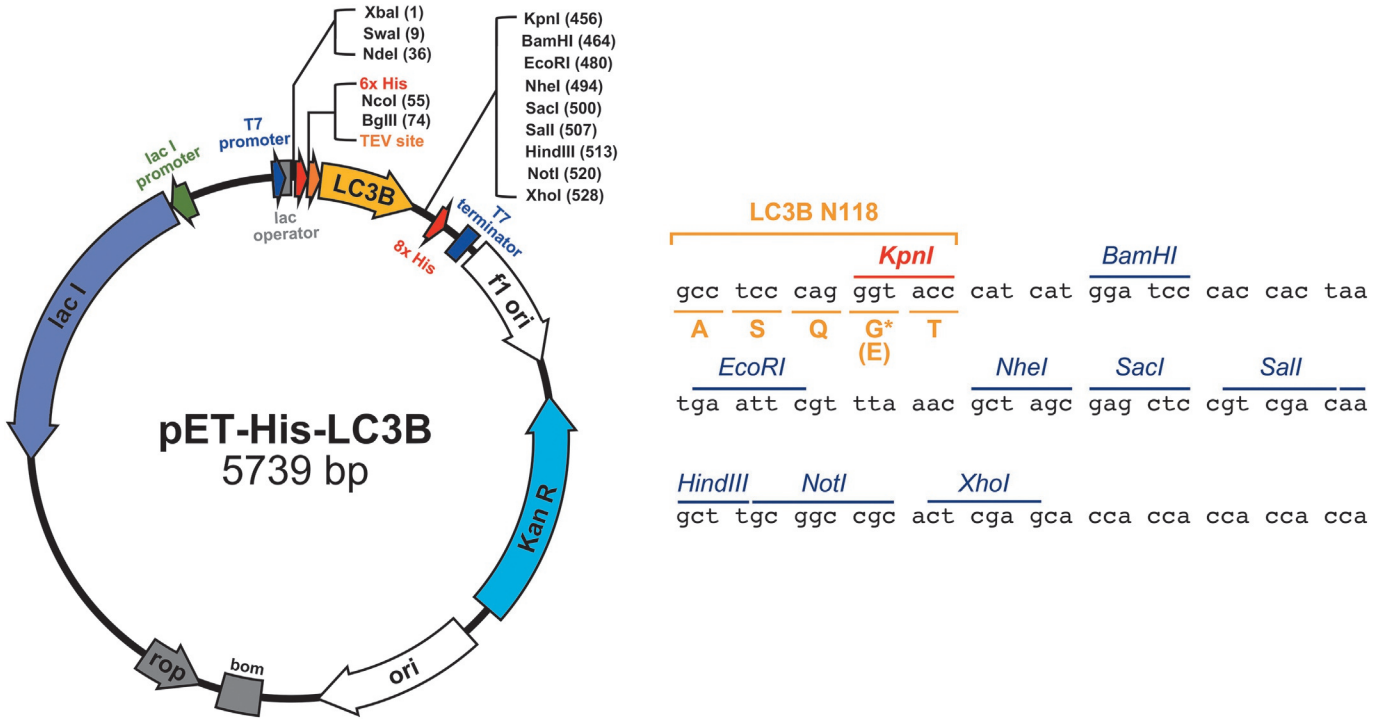

Fig. 2 Expression vector for the LC3B-fusion protein. The synthetic codon-optimized *LC3B* gene was inserted into the modified pET vector (Novagen) containing hexahistidine residues at the N-terminus. Immediately after the tag sequences is the TEV protease cleavage site. Multiple cloning sites begin at the *Kpn*I recognition sequence (456), and eight non-cleavable C-terminal histidine residues can be introduced before the *Xho*I recognition sequence (528) in the target protein depending on the construct design.

2. Key resources

2.1 Key resources table

Reagent or Resource	Source	Identifier
Bacterial Strains		
BL21(DE3) chemically competent cells	New England biolabs (NEB)	C2527H
Chemicals, Peptides, and Recombinant Proteins		
Trizma® base	Sigma-Aldrich	T1503
Sodium chloride	Sigma-Aldrich	S7653
Tris(2-carboxyethyl)phosphine hydrochloride	Sigma-Aldrich	C4706
Imidazole	Sigma-Aldrich	I202
Kanamycin sulfate	BioBasic	KB0286
MES monohydrate BioUltra, for molecular biology, ≥99.5%	Sigma-Aldrich	69889
Glycerol ReagentPlus®, ≥99.0% (GC)	Sigma-Aldrich	G7757
100% Polyethylene glycol 600	Hampton Research	HR2-859
50% w/v Polyethylene glycol 1000	Hampton Research	HR2-523
Deposited Data		
Structure of REEED-ZZ domain of p62	Protein Data Bank	5YP8
Structure of KEEED-ZZ domain of p62	Protein Data Bank	5YPA

Continued

—cont'd

Reagent or Resource	Source	Identifier
Structure of HEEED-ZZ domain of p62	Protein Data Bank	5YPB
Structure of FEEED-ZZ domain of p62	Protein Data Bank	5YPC
Structure of YEEED-ZZ domain of p62	Protein Data Bank	5YPE
Structure of WEEED-ZZ domain of p62	Protein Data Bank	5YPF
Structure of LEEED-ZZ domain of p62	Protein Data Bank	5YPG
Structure of IEEED-ZZ domain of p62	Protein Data Bank	5YPH
Oligonucleotides		
LC3B(**FG**)-*REEED*-p62 KpnI F (forward primer)	Integrated DNA Technologies	GCAA GGT ACC **TTC GGG** *CGT GAA GAA GAA GAT* GTG ATC TGC GAT GGC TGC AATG
LC3B(**FG**)-*REEED*-p62 XhoI R (reverse primer)	Integrated DNA Technologies	CCT GTC TGA GGG CTT CTC GTA ACT CGA GCA AG
Recombinant DNA		
Human LC3B gene	Integrated DNA Technologies	Fragment with human cDNA sequence encoding MAP1LC3B
Human ATG4B gene	Integrated DNA Technologies	gBlock gene fragment with human cDNA sequence encoding ATG4B
Software and Algorithms		
HKL2000 software package	HKL Research, Inc.	https://hkl-xray.com/
PHENIX software package	PHENIX	https://phenix-online.org/

2.2 Materials

- Sterile dH_2O
- KOD One™ PCR Master Mix (TOYOBO, Cat No. KMM-101)
- NucleoSpin® Gel and PCR Clean-up kit (Macherey-Nagel, Cat No. 740609.250)
- *Kpn*I-HF® restriction enzyme (NEB, Cat No. R3142S)
- *Xho*I restriction enzyme (NEB, Cat No. R0146S)
- Agarose, Type I, low EEO (Sigma-Aldrich, Cat No. A6013)
- Dyne LoadingSTAR, 6× conc. (Dyne Bio, Cat No. A750)
- Dyne 1 kb Plus DNA ladder, premixed with LoadingSTAR (Dyne Bio, Cat No. A750)
- rCutSmart Buffer, 10× conc. (NEB, Cat No. B6004S)
- T4 DNA Ligase (Roche, Cat No. 10716359001)
- Ligation buffer, 10× conc. (Roche, Cat No. 11243292001)
- BL21 DE3 competent cells (New England biolabs, Cat No. C2527H)
- LB broth low salt (Duchefa Biochemie, Cat No. L1703.0500)
- Agar, powder (JUNSEI, Cat No. 24440S1201)
- Kanamycin sulfate (BioBasic, Cat No. KB0286)
- Petri Dish, 90 × 15 mm (SPL life sciences, Cat No. 10090)
- 14 mL Round-Bottom Tube, 17 × 100 mm (SPL life sciences, Cat No. 40014)
- Exprep™ Plasmid SV mini (GeneAll®, Cat No. 101-102)
- Complete ULTRA Tablets, Mini, EDTA-free, *EASY*pack (Roche, Cat No. 05892791001)
- Ministart® Syringe Filter, 0.8 μm—NML, Hydrophilic (Sartorius, Cat No. 16592–K)
- Ministart® Syringe Filter, 0.45 μm—NML, Hydrophilic (Sartorius, Cat No. S6555–FMOSK)
- Ministart® Syringe Filter, 0.22 μm—NML, Hydrophilic (Sartorius, Cat No. S6534–FMOSK)
- HisTrap™ HP column, 5 mL (Cytiva, Cat No. 17524701)
- HiTrap™ Q HP column, 5 mL (Cytiva, Cat No. 17115301)
- HiLoad® 16/600 Superdex® 75 pg column (Cytiva, Cat No. 28-9893-33)
- VDX™ plate with sealant (Hampton Research Inc., Cat No. HR3-171)
- Siliconized Cover Slides Circles, 22 mm (Hampton Research Inc., Cat No. HR3-233)

2.3 Buffer recipes

- His A buffer (50 mM Tris base pH 8.0, 200 mM sodium chloride, 1 mM Tris(2-carboxyethyl)phosphine hydrochloride, in milli-Q water)
- His B buffer (50 mM Tris base pH 8.0, 100 mM sodium chloride, 500 mM imidazole, 1 mM Tris(2-carboxyethyl)phosphine hydrochloride, in milli-Q water)
- IEX A buffer (50 mM Tris base pH 8.0, 1 mM Tris(2-carboxyethyl) phosphine hydrochloride, in milli-Q water)
- IEX B buffer (50 mM Tris base pH 8.0, 1000 mM sodium chloride, 1 mM Tris(2-carboxyethyl)phosphine hydrochloride, in milli-Q water)
- SEC buffer (20 mM Tris base pH 8.0, 150 mM sodium chloride, 1 mM Tris(2-carboxyethyl)phosphine hydrochloride, in milli-Q water)
- REEED-crystallization solution (100 mM MES pH 6.0, 30% polyethylene glycol 600, 5% polyethylene glycol 1000, and 10% glycerol)

3. Preparation of N-degron attached ZZ-domain of p62/SQSTM1

This section describes the preparation of large amounts of N-degron fused ZZ-domain of p62/SQSTM1 (hereafter, ZZ-p62), an autophagy adapter (Cha-Molstad et al., 2015). The ZZ-domain is the N-degron recognition component of p62/SQSTM1, which binds to both type-1 (basic residues) and type-2 (bulky hydrophobic residues) N-degrons, and is different from the conventional UBR box and ClpS-homology domain (Cha-Molstad et al., 2017). Furthermore, the initial crystallization trial of ZZ-p62 was unsuccessful (Kwon et al., 2018). Therefore, we have developed the LC3B-fusion technique to design complex crystals with various N-degron residues and achieve better crystallization (Kim et al., 2020; Kwon et al., 2018).

3.1 Molecular cloning LC3B fused human p62 ZZ-domain

3.1.1 PCR amplification of ZZ-p62 (126-180)

(1) Mix 21 μL of sterile dH_2O, 1 μL of 10 ng/μL template DNA, 1.5 μL each of 10 μM forward and reverse primers (Note 1), and 25 μL of KOD One™ PCR Master Mix and make up to a total volume of 50 μL

(2) Thermocycler settings are as follows

(a) Initial denature step at 98 °C for 5 min—1 cycle

(b) Denature at 98 °C for 10 s, then anneal at 55 °C for 5 s, then elongate at 68 °C for 10 s when PCR product is smaller than 1 kb (Note 2)—30 cycles

(c) Final elongation step at 68 °C for 1 min—1 cycle

(3) PCR product is purified using NucleoSpin® Gel and PCR Clean-up kit following manufacturer's instructions. Elution volume is 43 μL

3.1.2 Digestion of insert PCR product

(1) Combine PCR product from Section 3.1.1 with 5 μL of 10× rCutSmart Buffer, and 1 μL each of *Kpn*I-HF® and *Xho*I restriction enzymes with a total volume of 50 μL (Note 3).

(2) Incubate the mixture for 1 h at 37 °C

(3) Purify the digested product as step 3, and the elution volume is 30 μL

3.1.3 Digestion of the pET-His-LC3B vector

(1) Mix 100 ng/μL of pET-His-LC3B vector (Fig. 2) with 3 μL of 10× rCutSmart Buffer, and 1 μL each of KpnI-HF® and XhoI restriction enzymes with a total volume of 30 μL

(2) Incubate the mixture for 1 h at 37 °C

(3) Purify the digested product as in Section 3.1.1 step 3, and the elution volume is 30 μL

3.1.4 Ligation

(1) Combine 10 μL of product from Section 3.1.2 step 3 and 7 μL of product from Section 3.1.3 step 3, add then 2 μL of 10× Ligation buffer and 1 μL of T4 DNA ligase

(2) Incubate the mixture for 1 h at 37 °C

3.1.5 Transformation

(1) Thaw BL21(DE3) competent cells (100 μL) on ice for 10 min, then add 20 μL of ligation product from 3.1.4.2 to cells near the alcohol lamp and incubate for 10 min on ice

(2) Heat shock cell at 42 °C for 1 min

(3) Incubate again on ice for 5 min, then add 650 μL of LB media to cells

(4) Incubate cell on thermomixer, the temperature of which is pre-set to 37 °C with 650 rpm agitation for 1 h

(5) Centrifuge cells at 2400×*g* for 3 min, drain 600 μL of supernatant. Resuspend cells and spread them onto LB agar plates containing 50 μg/mL kanamycin

(6) After 12 h, white colonies come up. Peak some of them with a sterile pipet tip and inoculate them into 1 mL of LB broth containing 50 μg/mL kanamycin with shaking for more than 6 h at 37 °C

3.1.6 Preparation of plasmids

(1) Pellet the cells *via* centrifugation at 17,000 × *g* for 1 min. Then, pour the supernatant entirely and purify the plasmids with Exprep™ Plasmid SV mini following the manufacturer's instructions

(2) Confirm the DNA sequence using sanger sequencing with universal primers T7 and T7 terminator (note 4)

3.1.7 Notes

(1) According to the desired N-terminal sequence preceding ZZ-p62. For these experiments, we used REEED_forward and REEED_reverse primers to expose the REEED sequence in the final protein. See the Section 2.1 key resource table for detailed sequence information

(2) When larger than 1 kb, use the elongation time of 10 s per kb

(3) For convenient cloning, the KpnI site was selected to insert the target gene into the vector. With the KpnI site, an additional sequence encoding Phe-Gly, corresponding to the 119–120 residue of LC3B, must be inserted before the target gene for cleaving the LC3B tag using ATG4B after expression. See the Section 2.1 key resource table for detailed sequence information

(4) DNA confirmed plasmid can be kept in −20 °C and used for transformation and other experiments later

3.2 Expression of N-degron fused ZZ-p62

3.2.1 Cell culture

(1) Seed one of the colonies whose sequence was confirmed at Section 3.1.6 step 2 to 5 mL of LB broth containing 50 μg/mL kanamycin (Note 1) and shake the tube for more than 16 h in the incubator at 160 rpm at 37 °C. Before the next step, prepare the autoclaved 800 mL LB broth in 2 L baffled flask

(2) Add 800 μL of 50 mg/mL kanamycin to 800 mL LB broth prepared in Section 3.2.1 step 1 to make a total concentration of 50 μg/mL. Then, inoculate 800 μL culture seed from Section 3.2.1 step 1 to this. Shake it for 6–8 h until OD_{600} reaches 0.7 at 160 rpm at 37 °C

(3) When OD_{600} of the culture from Section 3.2.1 step 2, cool it to 18 °C. We usually submerge it in water with ice for rapid cooling; this keeps the growth rate minimal while cooling

(4) After cooling, add 400 μL of 1 M of IPTG and 800 μL of 200 mM of $ZnCl_2$ to the culture to obtain a final concentration of 0.5 mM and 200 μM each (Note 2). Shake it for 18 h with 16 rpm at 18 °C

3.2.2 Cell harvest

(1) Divide cell culture from Section 3.2.1 step 3 into two 500 mL polypropylene bottles, and counterbalance the weight for centrifugation

(2) Centrifuge cells at 6000×*g* for 20 min

(3) You can see pellets of cells at the bottom of the bottles. Discard the entire supernatant and add 10 mL of His A buffer for cells from 800 mL culture (In this case, add 5 mL of His A buffer for each bottle).

(4) Resuspend the cell pellets with shaking at 200–250 rpm at 4 °C. After resuspending all the pellets, divide them into 50 mL conical tubes. Keep them at −20 °C for storage (Note 3).

3.2.3 Cell lysis

(1) After thawing cell suspension from Section 3.2.2 step 4, add one tablet of cocktail inhibitor (complete ULTRA Tablets, Mini, EDTA-free) and 1 mM of PMSF per 10 mL

(2) Lysis cells with ultrasonication. The ultrasonication settings are as follows when cells from the 2.4 L culture are used. Apply pulse (5 s of on time and 15 s of off time) for a total time of 6 min with 50% amplitude

(3) Centrifuge cell lysate at 35,000×*g* for 1 h, then collect only supernatant and filter it with 0.8, 0.45, and 0.2 μm sequentially

3.2.4 Notes

(1) All steps except cooling were conducted near the flame of the alcohol lamp to prevent contamination

(2) $ZnCl_2$ is added to help higher expression and proper folding of ZZ-p62 because it has zinc-binding motifs. For the expression of other proteins, $ZnCl_2$ addition is not necessary before IPTG induction

(3) We confirmed that cells could be kept at −20 °C for 6 months with almost no loss in protein quantity

(4) Ultrasonication setting could be different according to the number of cells to lysis and the status of the ultrasonifier. Cells are assumed to be completely disrupted when they seem much clearer

3.3 Purification of N-degron fused ZZ-p62

The overall purification scheme is depicted in Fig. 3. Although in this section, we used the example of REEED-fused ZZ-p62, a similar procedure can be used for all other N-degron fused proteins of interest. We have had similar results with the following proteins: yeast Nta1, human NTAQ1, human NTAN1, yeast Ate1, human UBR box from UBR1, UBR box from plant PRT6, and more.

3.3.1 His-affinity column chromatography

(1) Equilibrate 5 mL HisTrap™ HP column with 2% His B buffer (98% His A buffer +2% His B buffer).
(2) Load cell lysate from Section 3.2.3 step 3 to a pre-equilibrated column
(3) Wash the column with 2% His B buffer until the absorbance at 280 nm of loading through is unchanged (usually 50–100 mL in volume).
(4) Elute protein with 1–100% His B buffer gradient
(5) Wash the column with 50 mL His B buffer
(6) Wash the column with 50 mL His A buffer
(7) Wash the column with 50 mL 20% ethanol and store

3.3.2 Ion exchange column chromatography

(1) Equilibrate 5 mL HiTrap™ Q HP column with IEX A buffer
(2) Dilute elution from Section 3.3.1 step 4 threefold with IEX A buffer and load it onto the pre-equilibrated column
(3) Wash the column with IEX A buffer until the absorbance at 280 nm of loading through is unchanged (usually 50–100 mL in volume).
(4) Elute protein with 1–100% IEX B buffer
(5) Wash the column with 50 mL IEX B buffer
(6) Wash the column with 50 mL IEX A buffer
(7) Wash the column with 50 mL 20% ethanol and store

3.3.3 LC3B-tag cleavage and removal

(1) Treat 1/50 in a molar ratio of pure ATG4B enzyme (Section 4) to eluted sample from Section 3.3.2 step 4 and incubate overnight

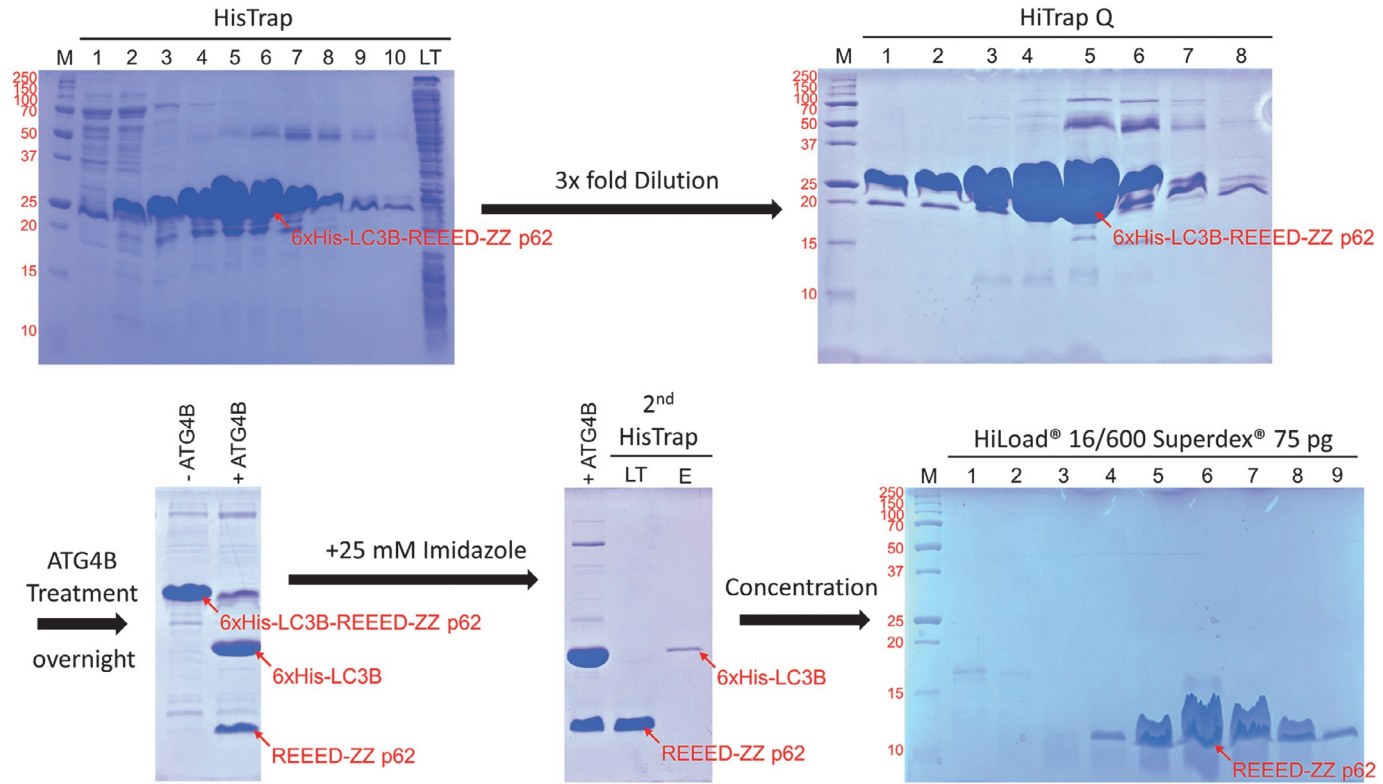

Fig. 3 Overall purification procedure of N-degron fused ZZ-p62. The basic chromatographic steps are His-affinity, anion exchange, and size exclusion. After Q-anion exchange column chromatography, the LC3B tag is cleaved by treating with ATG4B, following which the second His-affinity chromatography is performed to remove His-tagged LC3B and ATG4B.

(2) Equilibrate 5 mL HisTrap™ HP column with 30 mL 5% His B buffer
(3) Load sample from Section 3.3.3 step 1 onto a pre-equilibrated column and then wash 10 mL of 5% His B buffer to take all loaded samples out from the column. Collect all loading through
(4) Wash and store the column as given in Section 3.3.1 steps 5–7

3.3.4 Size exclusion chromatography

(1) Equilibrate the HiLoad® 16/600 Superdex® 75 pg column with SEC buffer
(2) Concentrate the loading through from Section 3.3.3 step 3 with 3 kDa MWCO Amicon® Ultra-15 Centrifugal Filter Unit at 2000×*g* and filter the concentrated sample with 0.22 μm Corning® Costar® Spin-X® centrifuge tube filters to remove aggregates arose during concentration
(3) Load the sample onto the equilibrated column and collect the eluted sample
(4) A typical elution profile and corresponding SDS-PAGE result are shown in Fig. 4

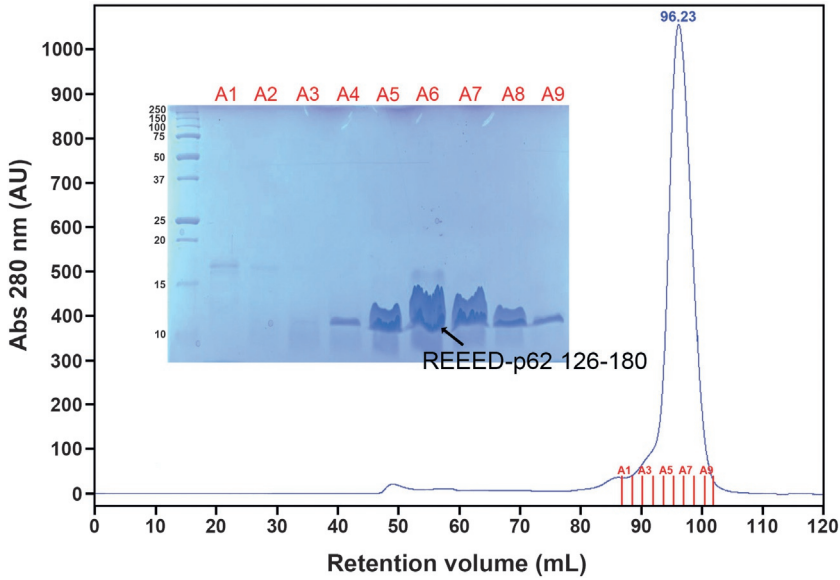

Fig. 4 An elution profile of size exclusion chromatography of N-degron fused ZZ-p62. Inset shows the SDS-PAGE results of the corresponding fractions of the elution profile. Based on the retention volume, the N-degron fused ZZ-p62 is a monomer in solution.

4. Preparation of human ATG4B protease

Gene encoding full-length human ATG4B is amplified from human cDNA and cloned into a conventional pET vector to have N-terminal 6× His tag using restriction enzyme sites BamHI and *Xho*I. The process and condition of cell culture to lysis are identical to that described in REEED-ZZ p62 in Section 3. The preparation of ATG4B protease was reported previously (Kwon, Kim, Jung, et al., 2017), and in the following part, the procedure after cell lysis is described.

4.1 Purification of human ATG4B

4.1.1 His-affinity column chromatography

(1) Equilibrate 5 mL HisTrap™ HP column with 2% His B buffer (98% His A buffer +2% His B buffer)
(2) Load cell lysate to the pre-equilibrated column
(3) Wash the column with 2% His B buffer until the absorbance at 280 nm of loading through is unchanged (Usually 50–100 mL in volume)
(4) Elute protein with 1–100%/80 min His B buffer gradient
(5) Wash the column as given in Section 3.3.1 steps 5–7 and store it

4.1.2 Ion exchange column chromatography

(1) Equilibrate 5 mL HiTrap™ Q HP column with IEX A buffer
(2) Dilute elution from Section 4.1.1 step 4 with 3× fold with IEX A buffer and load it onto the pre-equilibrated column
(3) Wash the column with IEX A buffer until the absorbance at 280 nm of loading through is unchanged (usually 50–100 mL in volume).
(4) Elute protein with 1–100%/80 min IEX B buffer. Human ATG4B may be eluted with two peaks in Q HP, but we use only the second peak eluted with higher concentration B, because this peak is more definite and seem to cleave LC3B more efficiently
(5) Wash the column as given in Section 3.3.1 steps 5–7 and store it
(6) Check the concentration of the eluted sample from Section 4.1.2 step 4 and make 500 μL volume of aliquot. Flash freeze these aliquots with liquid nitrogen and keep them in deep freezer at −80 °C. Thaw this aliquot and use as much as you need to purify LC3B fused protein

5. Applications of N-degron fused ZZ-p62 or N-degron fused proteins of interest

5.1 Crystallization of REEED-ZZ p62

(1) Concentrate the eluted sample from Section 3.3.4 step 3 using 3 kDa MWCO Amicon® Ultra-15 Centrifugal Filter Unit with 2000×*g* to 15 mg/mL and filter the concentrated sample with 0.22 μm Corning® Costar® Spin-X® centrifuge tube filters

(2) Aliquot 500 μL of REEED-crystallization solution in each well of VDX™ plate (Note 1).

(3) Prepare cover slide circles and place 1 μL of the same crystallization buffer in the center of the cover slide and immediately mix 1 μL of the protein sample from Section 5.1 step 1

(4) Flip and gently cover the slides with the solution mixture to the sealant around each well of the VDX™ plate. Complete sealing, with no air bubbles, is essential in this step

(5) The crystal grows usually within 24 h (Notes 2 and 3).

(6) Fully-grown crystal is transferred to the same REEED-crystallization solution with 30% glycerol concentration for cryo-protection. The crystal was flash-frozen in liquid nitrogen

5.2 Notes

(1) Making different ratios of ingredients for the crystallization solution in each well is helpful to optimize the crystallization. Because the environment of the crystallization room could differ with each lab, optimization of own crystallization condition is important to get a good quality crystal

(2) Crystals of different proteins other than REEED-ZZ p62 grow in different conditions and thus, diverse crystallization conditions must be screened

(3) In the case of N-degron fused ZZ-p62, the initial screen provided more than 200 crystals among 1632 different crystallization conditions using commercially available kits. Several representative crystals are shown in Fig. 5 and their detailed conditions are listed in the figure legend

5.3 Structure determination

The diffraction experiment of crystals was done at Synchrotron facilities, and the data was processed using programs HKL2000 (Otwinowski &

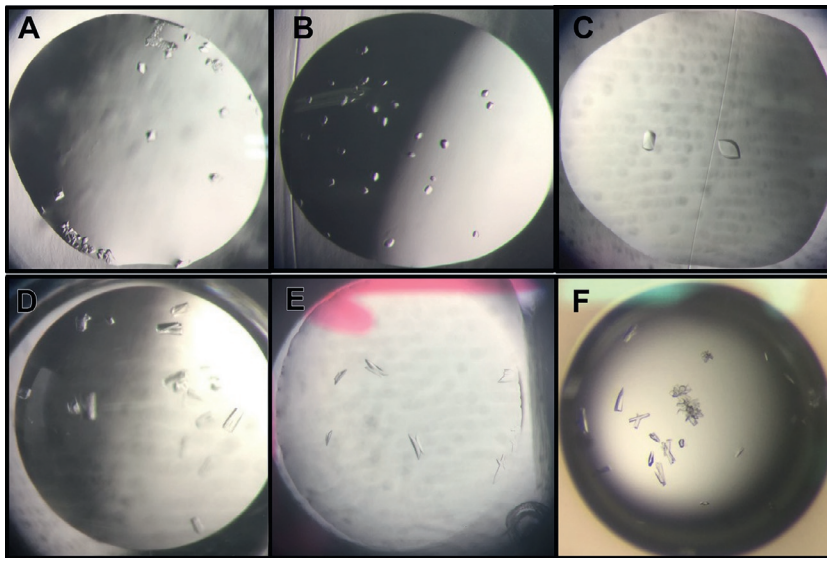

Fig. 5 Crystals of N-degron bound-ZZ domain of p62/SQSTM1. Photograph of various crystals conditions (A–F). Crystallization conditions are as follows: (A) 100 mM Tris-HCl pH 7.0, 200 mM magnesium chloride, 50% (*v*/v) ethylene glycol; (B) 100 mM sodium citrate pH 5.5, 5% (*w*/*v*) PEG 3000, 35% (v/v) 1,2-propanediol; (C) 100 mM MES-NaOH pH 6.0, 5% (w/v) PEG 1000, 30% (v/v) PEG 600, 10% (v/v) glycerol; (D) 100 mM Bis-Tris pH 5.5, 100 mM ammonium sulfate, 17% (w/v) polyethylene glycol 10,000; (E) 100 mM Buffer System 2 pH 7.5, 0.06 M Divalents, 37.5% (v/v) Precipitant Mix 4 [Buffer System 2: Na-HEPES, MOPS (acid); Divalents: 0.3 M magnesium chloride hexahydrate, 0.3 M calcium chloride dehydrate; 75% Precipitant Mix 4: 25% (v/v) MPD, 25% (w/v) PEG 1000, 25% (w/v) PEG 3350]; (F) 100 mM BIS-TRIS pH 5.5, 25% (w/v) PEG 3350.

Minor, 1997) and PHENIX (Adams et al., 2010). Using this method, we could determine the structure of REEED-ZZ p62 at 1.45 Å resolution (Kwon et al., 2018) and we observed the electron density map of N-terminal REEED bound to the binding pocket in neighboring molecules of ZZ-p62, which helps the crystal packing (Fig. 1). Using a modification of this method, we also could obtain the purified proteins with different N-terminal residues. To verify the N-termini of the purified proteins, we performed the N-terminal sequencing using Edman degradation. Furthermore, we successfully obtained crystals of human ZZ-p62 with various N-degrons such as REEED, KEEED, HEEED, FEEED, YEEED, WEEED, LEEED, and IEEED using the method described in this chapter and all structures were determined (Fig. 6).

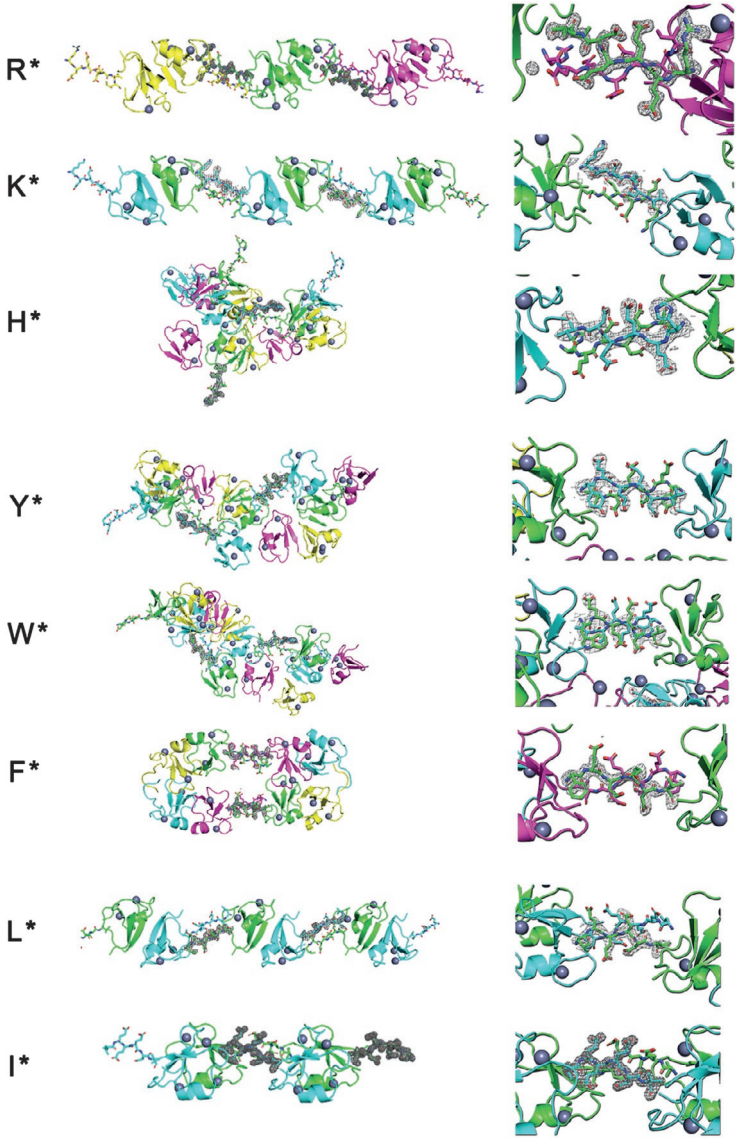

Fig. 6 Structures of various N-degron complexed ZZ-p62. The N-degron residues protrude from the ZZ-domain core and bind to the neighboring symmetry-equivalent molecule in different modes of crystal packing. Close-up views on the right show the electron density maps of N-degron segments from the symmetry-equivalent molecules. The electron density map for this region is clear enough for model building, and there is no invisible region.

5.4 Other applications of LC3B-fusion technique

We described the procedures for preparing the N-degron fused ZZ-p62 in this chapter. With this technique, we could test many biochemical characteristics of proteins in the N-degron pathway. A few examples include: (1) The arginylated BiP, a substrate of p62/SQSTM1 was successfully produced and verified using the antibody for detecting N-terminal arginine residue (Cha-Molstad et al., 2017; Kim et al., 2020). (2) Leucylated GFP is a model substrate for various applications. We used this protein for studying type-2 N-recognin (Kim et al., 2020; Kim et al., 2021). The purified *E. coli* ClpS protein was used for making an affinity column to fish out the *in vivo* substrates of N-degron pathway. The leucylated GFP is a positive control for this column. (3) The enzymes we produced using this method are enzymatically competent. For example, when the yeast Nta1, N-terminal demidase, was overexpressed and fused with its substrate residues (Asn or Gln) at the N-terminus, the N-terminus of the purified protein contained Asp or Glu residues, which are an enzyme reaction products (Kim et al., 2020; Kim, Oh, et al., 2016).

6. Conclusions

In this chapter, we described a method for producing proteins of interest that possess the N-degron sequence. The N-degron fused to the N-termini of target proteins has now been successfully applied to crystallize proteins in the N-degron pathway, not only to increase crystal quality but also to yield complex structures (Figs. 1 and 6). As was described in Section 1, the LC3B-fusion technique plus a standard expression with Met-Pro sequence can produce all 20 different N-degron sequences (Fig. 1). Therefore, the application of this technique for N-degron *in vitro* research is almost unlimited.

Acknowledgments

We thank all members of the Song Laboratory for their valuable input. This study was supported by National Research Foundation of Korea (NRF) grants from the Korean government (Grant Nos. 2020R1A2C3008285, 2021M3A9I4030068, and 2022M3A9G8082638).

References

Adams, P. D., Afonine, P. V., Bunkoczi, G., Chen, V. B., Davis, I. W., Echols, N., et al. (2010). PHENIX: A comprehensive Python-based system for macromolecular structure solution. *Acta Crystallographica. Section D, Biological Crystallography*, *66*(Pt 2), 213–221. https://doi.org/10.1107/S0907444909052925.

Aksnes, H., Drazic, A., Marie, M., & Arnesen, T. (2016). First things first: Vital protein marks by N-terminal acetyltransferases. *Trends in Biochemical Sciences*, *41*(9), 746–760. https://doi.org/10.1016/j.tibs.2016.07.005.

Bachmair, A., Finley, D., & Varshavsky, A. (1986). In vivo half-life of a protein is a function of its amino-terminal residue. *Science*, *234*(4773), 179–186. https://doi.org/10.1126/science.3018930.

Bachmair, A., & Varshavsky, A. (1989). The degradation signal in a short-lived protein. *Cell*, *56*(6), 1019–1032. https://doi.org/10.1016/0092-8674(89)90635-1.

Baker, R. T. (1996). Protein expression using ubiquitin fusion and cleavage. *Current Opinion in Biotechnology*, *7*(5), 541–546. https://doi.org/10.1016/s0958-1669(96)80059-0.

Baker, R. T., & Varshavsky, A. (1995). Yeast N-terminal amidase. A new enzyme and component of the N-end rule pathway. *The Journal of Biological Chemistry*, *270*(20), 12065–12074. https://doi.org/10.1074/jbc.270.20.12065.

Balzi, E., Choder, M., Chen, W. N., Varshavsky, A., & Goffeau, A. (1990). Cloning and functional analysis of the arginyl-tRNA-protein transferase gene ATE1 of *Saccharomyces cerevisiae*. *The Journal of Biological Chemistry*, *265*(13), 7464–7471. Retrieved from https://www.ncbi.nlm.nih.gov/pubmed/2185248.

Berrade, L., & Camarero, J. A. (2009). Expressed protein ligation: A resourceful tool to study protein structure and function. *Cellular and Molecular Life Sciences*, *66*(24), 3909–3922. https://doi.org/10.1007/s00018-009-0122-3.

Cha-Molstad, H., Sung, K. S., Hwang, J., Kim, K. A., Yu, J. E., Yoo, Y. D., et al. (2015). Amino-terminal arginylation targets endoplasmic reticulum chaperone BiP for autophagy through p62 binding. *Nature Cell Biology*, *17*(7), 917–929. https://doi.org/10.1038/ncb3177.

Cha-Molstad, H., Yu, J. E., Feng, Z., Lee, S. H., Kim, J. G., Yang, P., et al. (2017). p62/SQSTM1/Sequestosome-1 is an N-recognin of the N-end rule pathway which modulates autophagosome biogenesis. *Nature Communications*, *8*(1), 102. https://doi.org/10.1038/s41467-017-00085-7.

Chen, S. J., Kim, L., Song, H. K., & Varshavsky, A. (2021). Aminopeptidases trim Xaa-Pro proteins, initiating their degradation by the Pro/N-degron pathway. *Proceedings of the National Academy of Sciences of the United States of America*, *118*(43). https://doi.org/10.1073/pnas.2115430118.

Chen, S. J., Wu, X., Wadas, B., Oh, J. H., & Varshavsky, A. (2017). An N-end rule pathway that recognizes proline and destroys gluconeogenic enzymes. *Science*, *355*(6323). https://doi.org/10.1126/science.aal3655.

Choi, W. S., Jeong, B. C., Joo, Y. J., Lee, M. R., Kim, J., Eck, M. J., et al. (2010). Structural basis for the recognition of N-end rule substrates by the UBR box of ubiquitin ligases. *Nature Structural & Molecular Biology*, *17*(10), 1175–1181. https://doi.org/10.1038/nsmb.1907.

Chrustowicz, J., Sherpa, D., Teyra, J., Loke, M. S., Popowicz, G. M., Basquin, J., et al. (2022). Multifaceted N-degron recognition and ubiquitylation by GID/CTLH E3 ligases. *Journal of Molecular Biology*, *434*(2), 167347. https://doi.org/10.1016/j.jmb.2021.167347.

Dong, C., Chen, S. J., Melnykov, A., Weirich, S., Sun, K., Jeltsch, A., et al. (2020). Recognition of nonproline N-terminal residues by the Pro/N-degron pathway. *Proceedings of the National Academy of Sciences of the United States of America*, *117*(25), 14158–14167. https://doi.org/10.1073/pnas.2007085117.

Dong, C., Zhang, H., Li, L., Tempel, W., Loppnau, P., & Min, J. (2018). Molecular basis of GID4-mediated recognition of degrons for the Pro/N-end rule pathway. *Nature Chemical Biology*, *14*(5), 466–473. https://doi.org/10.1038/s41589-018-0036-1.

Hong, S. B., Kim, B. W., Kim, J. H., & Song, H. K. (2012). Structure of the autophagic E2 enzyme Atg10. *Acta Crystallographica. Section D, Biological Crystallography*, *68*(Pt 10), 1409–1417. https://doi.org/10.1107/S0907444912034166.

Hong, S. B., Kim, B. W., Lee, K. E., Kim, S. W., Jeon, H., Kim, J., et al. (2011). Insights into noncanonical E1 enzyme activation from the structure of autophagic E1 Atg7 with Atg8. *Nature Structural & Molecular Biology*, *18*(12), 1323–1330. https://doi.org/10.1038/nsmb.2165.

Hu, R. G., Wang, H., Xia, Z., & Varshavsky, A. (2008). The N-end rule pathway is a sensor of heme. *Proceedings of the National Academy of Sciences of the United States of America*, *105*(1), 76–81. https://doi.org/10.1073/pnas.0710568105.

Hwang, C. S., Shemorry, A., & Varshavsky, A. (2010). N-terminal acetylation of cellular proteins creates specific degradation signals. *Science*, *327*(5968), 973–977. https://doi.org/10.1126/science.1183147.

Hwang, C. S., & Varshavsky, A. (2008). Regulation of peptide import through phosphorylation of Ubr1, the ubiquitin ligase of the N-end rule pathway. *Proceedings of the National Academy of Sciences of the United States of America*, *105*(49), 19188–19193. https://doi.org/10.1073/pnas.0808891105.

Kim, L., Heo, J., Kwon, D. H., Shin, J. S., Jang, S. H., Park, Z. Y., et al. (2021). Structural basis for the N-degron specificity of ClpS1 from Arabidopsis thaliana. *Protein Science*, *30*(3), 700–708. https://doi.org/10.1002/pro.4018.

Kim, H. K., Kim, R. R., Oh, J. H., Cho, H., Varshavsky, A., & Hwang, C. S. (2014). The N-terminal methionine of cellular proteins as a degradation signal. *Cell*, *156*(1–2), 158–169. https://doi.org/10.1016/j.cell.2013.11.031.

Kim, B. H., Kim, M. K., Oh, S. J., Nguyen, K. T., Kim, J. H., Varshavsky, A., et al. (2022). Crystal structure of the Ate1 arginyl-tRNA-protein transferase and arginylation of N-degron substrates. *Proceedings of the National Academy of Sciences of the United States of America*, *119*(31). https://doi.org/10.1073/pnas.2209597119.

Kim, L., Kwon, D. H., Heo, J., Park, M. R., & Song, H. K. (2020). Use of the LC3B-fusion technique for biochemical and structural studies of proteins involved in the N-degron pathway. *The Journal of Biological Chemistry*, *295*(9), 2590–2600. https://doi.org/10.1074/jbc.RA119.010912.

Kim, B. W., Kwon, D. H., & Song, H. K. (2016). Structure biology of selective autophagy receptors. *BMB Reports*, *49*(2), 73–80. https://doi.org/10.5483/bmbrep.2016.49.2.265.

Kim, M. K., Oh, S. J., Lee, B. G., & Song, H. K. (2016). Structural basis for dual specificity of yeast N-terminal amidase in the N-end rule pathway. *Proceedings of the National Academy of Sciences of the United States of America*, *113*(44), 12438–12443. https://doi.org/10.1073/pnas.1612620113.

Kim, J. M., Seok, O. H., Ju, S., Heo, J. E., Yeom, J., Kim, D. S., et al. (2018). Formyl-methionine as an N-degron of a eukaryotic N-end rule pathway. *Science*, *362*(6418). https://doi.org/10.1126/science.aat0174.

Kwon, D. H., Kim, S., Jung, Y. O., Roh, K. H., Kim, L., Kim, B. W., et al. (2017). The 1:2 complex between RavZ and LC3 reveals a mechanism for deconjugation of LC3 on the phagophore membrane. *Autophagy*, *13*(1), 70–81. https://doi.org/10.1080/15548627.2016.1243199.

Kwon, D. H., Kim, L., Kim, B. W., Kim, J. H., Roh, K. H., Choi, E. J., et al. (2017). A novel conformation of the LC3-interacting region motif revealed by the structure of a complex between LC3B and RavZ. *Biochemical and Biophysical Research Communications*, *490*(3), 1093–1099. https://doi.org/10.1016/j.bbrc.2017.06.173.

Kwon, D. H., Kim, L., & Song, H. K. (2019). pH-dependent regulation of SQSTM1/p62 during autophagy. *Autophagy*, *15*(1), 180–181. https://doi.org/10.1080/15548627.2018.1532264.

Kwon, D. H., Park, O. H., Kim, L., Jung, Y. O., Park, Y., Jeong, H., et al. (2018). Insights into degradation mechanism of N-end rule substrates by p62/SQSTM1 autophagy adapter. *Nature Communications*, *9*(1), 3291. https://doi.org/10.1038/s41467-018-05825-x.

Kwon, D. H., & Song, H. K. (2018). A structural view of xenophagy, a battle between host and microbes. *Molecules and Cells*, *41*(1), 27–34. https://doi.org/10.14348/molcells.2018.2274.

Maruyama, T., & Noda, N. N. (2017). Autophagy-regulating protease Atg4: Structure, function, regulation and inhibition. *Journal of Antibiotics (Tokyo)*, *71*(1), 72–78. https://doi.org/10.1038/ja.2017.104.

Matta-Camacho, E., Kozlov, G., Li, F. F., & Gehring, K. (2010). Structural basis of substrate recognition and specificity in the N-end rule pathway. *Nature Structural & Molecular Biology*, *17*(10), 1182–1187. https://doi.org/10.1038/nsmb.1894.

Metlagel, Z., Otomo, C., Ohashi, K., Takaesu, G., & Otomo, T. (2014). Structural insights into E2-E3 interaction for LC3 lipidation. *Autophagy*, *10*(3), 522–523. https://doi.org/10.4161/auto.27594.

Munoz-Escobar, J., Kozlov, G., & Gehring, K. (2017). Crystal structure of the UBR-box from UBR6/FBXO11 reveals domain swapping mediated by zinc binding. *Protein Science*, *26*(10), 2092–2097. https://doi.org/10.1002/pro.3227.

Nakatogawa, H., Suzuki, K., Kamada, Y., & Ohsumi, Y. (2009). Dynamics and diversity in autophagy mechanisms: Lessons from yeast. *Nature Reviews. Molecular Cell Biology*, *10*(7), 458–467. https://doi.org/10.1038/nrm2708.

Nguyen, K. T., Kim, J. M., Park, S. E., & Hwang, C. S. (2019). N-terminal methionine excision of proteins creates tertiary destabilizing N-degrons of the Arg/N-end rule pathway. *The Journal of Biological Chemistry*, *294*(12), 4464–4476. https://doi.org/10.1074/jbc.RA118.006913.

Noda, N. N., Ohsumi, Y., & Inagaki, F. (2010). Atg8-family interacting motif crucial for selective autophagy. *FEBS Letters*, *584*(7), 1379–1385. https://doi.org/10.1016/j.febslet.2010.01.018.

Ohsumi, Y. (2001). Molecular dissection of autophagy: Two ubiquitin-like systems. *Nature Reviews. Molecular Cell Biology*, *2*(3), 211–216. https://doi.org/10.1038/35056522.

Otwinowski, Z., & Minor, W. (1997). Processing of X-ray diffraction data collected in oscillation mode. *Methods in Enzymology*, *276*, 307–326. Retrieved from https://www.ncbi.nlm.nih.gov/pubmed/27754618.

Pan, M., Zheng, Q., Wang, T., Liang, L., Mao, J., Zuo, C., et al. (2021). Structural insights into Ubr1-mediated N-degron polyubiquitination. *Nature*, *600*(7888), 334–338. https://doi.org/10.1038/s41586-021-04097-8.

Park, S. W., Jeon, P., Yamasaki, A., Lee, H. E., Choi, H., Mun, J. Y., et al. (2022). Development of new tools to study membrane-anchored mammalian Atg8 proteins. *Autophagy*, *1-20*. https://doi.org/10.1080/15548627.2022.2132040.

Piatkov, K. I., Vu, T. T., Hwang, C. S., & Varshavsky, A. (2015). Formyl-methionine as a degradation signal at the N-termini of bacterial proteins. *Microbial Cell*, *2*(10), 376–393. https://doi.org/10.15698/mic2015.10.231.

Qiao, S., Langlois, C. R., Chrustowicz, J., Sherpa, D., Karayel, O., Hansen, F. M., et al. (2020). Interconversion between anticipatory and active GID E3 ubiquitin ligase conformations via metabolically driven substrate receptor assembly. *Molecular Cell*, *77*(1), 150–163 e159. https://doi.org/10.1016/j.molcel.2019.10.009.

Satakarni, M., & Curtis, R. (2011). Production of recombinant peptides as fusions with SUMO. *Protein Expression and Purification*, *78*(2), 113–119. https://doi.org/10.1016/j.pep.2011.04.015.

Satoo, K., Noda, N. N., Kumeta, H., Fujioka, Y., Mizushima, N., Ohsumi, Y., et al. (2009). The structure of Atg4B-LC3 complex reveals the mechanism of LC3 processing and delipidation during autophagy. *The EMBO Journal*, *28*(9), 1341–1350. https://doi.org/10.1038/emboj.2009.80.

Schaaf, M. B., Keulers, T. G., Vooijs, M. A., & Rouschop, K. M. (2016). LC3/GABARAP family proteins: Autophagy-(un)related functions. *The FASEB Journal*, *30*(12), 3961–3978. https://doi.org/10.1096/fj.201600698R.

Shemorry, A., Hwang, C. S., & Varshavsky, A. (2013). Control of protein quality and stoichiometries by N-terminal acetylation and the N-end rule pathway. *Molecular Cell*, *50*(4), 540–551. https://doi.org/10.1016/j.molcel.2013.03.018.

Sherpa, D., Chrustowicz, J., & Schulman, B. A. (2022). How the ends signal the end: Regulation by E3 ubiquitin ligases recognizing protein termini. *Molecular Cell*, *82*(8), 1424–1438. https://doi.org/10.1016/j.molcel.2022.02.004.

Shin, J. S., Park, S. H., Kim, L., Heo, J., & Song, H. K. (2021). Crystal structure of yeast Gid10 in complex with Pro/N-degron. *Biochemical and Biophysical Research Communications*, *582*, 86–92. https://doi.org/10.1016/j.bbrc.2021.10.007.

Tanida, I., Ueno, T., & Kominami, E. (2004). LC3 conjugation system in mammalian autophagy. *The International Journal of Biochemistry & Cell Biology*, *36*(12), 2503–2518. https://doi.org/10.1016/j.biocel.2004.05.009.

Tasaki, T., & Kwon, Y. T. (2007). The mammalian N-end rule pathway: New insights into its components and physiological roles. *Trends in Biochemical Sciences*, *32*(11), 520–528. https://doi.org/10.1016/j.tibs.2007.08.010.

Van Damme, P., Osberg, C., Jonckheere, V., Glomnes, N., Gevaert, K., Arnesen, T., et al. (2022). Expanded in vivo substrate profile of the yeast N-terminal acetyltransferase NatC. *The Journal of Biological Chemistry*, *102824*. https://doi.org/10.1016/j.jbc.2022.102824.

Varshavsky, A. (2008). Discovery of cellular regulation by protein degradation. *The Journal of Biological Chemistry*, *283*(50), 34469–34489. https://doi.org/10.1074/jbc.X800009200.

Varshavsky, A. (2019). N-degron and C-degron pathways of protein degradation. *Proceedings of the National Academy of Sciences of the United States of America*, *116*(2), 358–366. https://doi.org/10.1073/pnas.1816596116.

Xiao, Q., Zhang, F., Nacev, B. A., Liu, J. O., & Pei, D. (2010). Protein N-terminal processing: Substrate specificity of *Escherichia coli* and human methionine aminopeptidases. *Biochemistry*, *49*(26), 5588–5599. https://doi.org/10.1021/bi1005464.